Crustal Heat Flow Variations of in the Equatorial Atlantic: Implications for geothermal structure of NE Brazil

Roberto R. Cardoso and Valiya M. Hamza – Observatório Nacional - ON/MCT, Rio de Janeiro

Abstract

The results of a recent reappraisal of crustal heat flow data for the equatorial region of the Atlantic Ocean are presented. The main purpose has been the comparison of large scale variations in thermal field of ocean floor with the trends discernible in harmonic representation of the global heat flow pattern. The results obtained reveal that the harmonic representation based on 12 degree expansion lacks the spatial resolution needed for identifying local anomalies. Attempts to remedy this problem with use of synthetic values derived from plate cooling theory, a practice adopted in deriving the global heat flow map of 1993, is found to lead to severe distortions in the heat flow field on local and regional scales. On the other hand, harmonic representation based on 36 degree expansion, without the use of synthetic values, is found to provide a reasonable representation of the regional heat flow. We conclude that use of synthetic values for representing regional scale features in heat flow distribution leads to undesirable consequences and is unwarranted.

Introduction

Determining regional scale features in heat flow is often considered an important step in the analysis of local variations of the geothermal field. In the present work we make use of the heat flow data derived from the global compilation, set up by the International Heat Flow Commission – IHFC, in outlining the regional scale features in the crustal geothermal field of the equatorial Atlantic. This area was selected because of the availability of a reasonably large number of heat flow measurements and its fairly homogeneous geographic distribution.

Two different approaches were adopted in the present work for examining large scale variations. The first one is based on the published set of spherical harmonic coefficients, used for representing the global heat flow pattern. Though the spherical harmonic expansion filters out short wavelength components the coefficients can still be employed in determining the regional field. The second approach is based on the use of experimental data sets for generating a numerical representation of the regional field. An alternative is to make use of the well known methods of trend surface analysis (Vasseur and Nouri, 1980;, Hamza et al, 2005). Comparative analysis of the results obtained by these approaches is considered to be a potentially useful tool in understanding the nature of large scale variations of heat flow through the ocean crust and also in assessment of global heat loss.

Heat flow Data for the Equatorial Atlantic

According to the global heat flow data base, available for download at the web site of the National Geophysical Data Center (NGDC), there are a total of 1241 records of heat flow measurements in the Atlantic ocean. Of these nearly 400 are in the equatorial region, over 600 are in the Northern parts and the remaining ones in the southern parts.

The overall geographic distribution of heat flow data over the Atlântic Ocean is illustrated in Figure (1). The availability of data is poor in several of the major regional sectors and geotectonic units of the northern and southern sectors of the Atlantic and also in the Polar Regions. The data density is relatively better in the central region but the distribution is relatively heterogeneous.

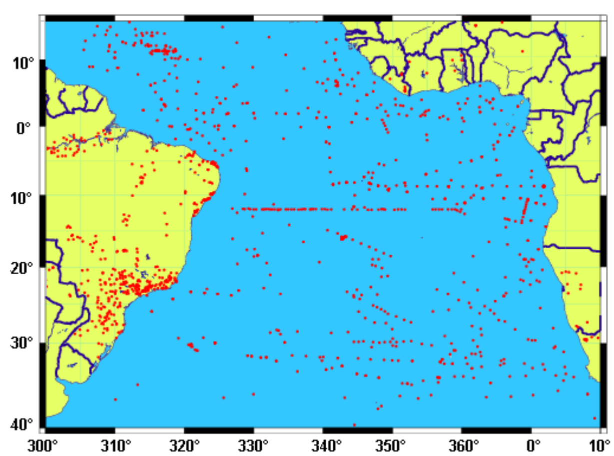

Figure (1) Distribution of heat flow data in the central parts of the Atlantic Ocean and in the neighboring areas.

A summary of the mean heat flow values and the respective standard deviations for the 14 main regions of the Atlantic Ocean is given in Table (1). As can be seen from this table the mean values fall in the range of 40 to 165mW/m^2. However, the mean heat flow is less than

80mW/m^2 in 10 out of the 14 regional structures. In fact high mean values are found only in sectors that enclose active segments of the mid ocean ridges. Icelandic region is a typical example. On the other hand regions that are away from the main ridge areas are found to have low to normal heat flow values (in the range of 40 to 80mW/m^2).

The large variations in heat flow values nakes the analysis of regional trends a difficult task. Mapping heat flow fields on a regional scale is one form of minimizing problems arising from non-homogeneous distribution. However features revealed in such maps are to a large extent dependent on the density and distribution of the primary data used in the analysis.

Table (1) Summary of heat flow values for the different regions of the Atlantic Ocean. N is number of data and σ mean deviation.

Region	N	Heat Flow (mW/m^2) Mean	σ
Mid Caribbean	19	62,4	36,4
I M V	19	52,7	17,5
Central Atlantic	198	66,7	35,9
Caribbean	24	144,2	63,1
Caribbean Atlantic	40	85,1	49,9
Mexican Gulf	72	50,5	14,1
Iceland	27	165,3	65,9
East of Canada	16	40,3	11,0
Mid Atlantic	251	62,8	29,0
North Atlantic	234	101,4	73,6
Reykjanes area	52	76,9	28,7
South Atlantic	15	78,6	58,7
West of Africa	261	65,7	26,6
West Atlantic	13	66,3	16,7
Total	1241	75,5	37,6

Regional Trends in the global heat flow map of 1993

The large scale features present in global heat flow maps provide an opportunity for understanding the nature of regional variations. For obvious reasons spherical harmonic analysis has been the preferred method employed in deriving global heat flow maps. In the earlier attempts (see for example, Lee and MacDonald, 1963, Lee and Uyeda, 1965; Horai and Simmons, 1969) the procedure adopted has been based on methods that make use of experimental data in generating an over determined set of equations, which in turn is solved for the unknown coefficients. This approach has the inherent weakness that the coefficients are sensitive to changes in data density. In the later work by Chapman and Pollack (1975) problems arising from uneven data distribution were minimized by calculating mean heat flow values over a surface grid system of 5^0 x 5^0. In addition, they employed estimated values of heat flow for those area elements for which experimental data were not available. Empirical predictors, based on the well-known heat flow-age relation (Polyak and Smirnov, 1968; Hamza and Verma, 1969), were employed in obtaining estimated values.

The technique of spherical harmonic expansion is well known. The basic theory of the method is outlined in the Appendix. The global heat flow map of Chapman and Pollack (1975) is based on a 12 degree expansion of the harmonic representation.

Pollack et al (1993) also adopted a procedure somewhat similar to that of the earlier work by Chapman and Pollack (1975). In spite of considerable improvements in the database the global map of Pollack et al (1975) is limited to a 12 degree expansion of the harmonic representation. However, some significant modifications were introduced in the use of empirical predictors. For example, results of heat flow measurements in the mid-ocean ridge areas were rejected based on the ad-hoc argument that the experimental data does not take into account the effects of convective heat transfer by hydrothermal circulation. Instead, they opted in favor of use of theoretical heat flow values calculated on the basis of plate cooling models as substitute for experimental data.

In the present work the set of harmonic coefficients calculated by Pollack et al (1993) were used in deriving the regional heat flow pattern in the equatorial region of the Atlantic Ocean. The results obtained are presented in the map of figure (3). The map is rather smooth because the harmonic representation has filtered out short wavelength variations. However, the most striking feature of the harmonic representation of Pollack et al (1993) is the rather very broad heat flow anomaly (with values in excess of 80mW/m^2) over much of the oceanic crust in the central Atlantic. Heat flow values in the range of 30 to 60 mW/m^2 are found only along very narrow belts, close to the continental margins. Needless to say such features are in direct contradiction with the experimental data set and the mean values calculated in Table (1).

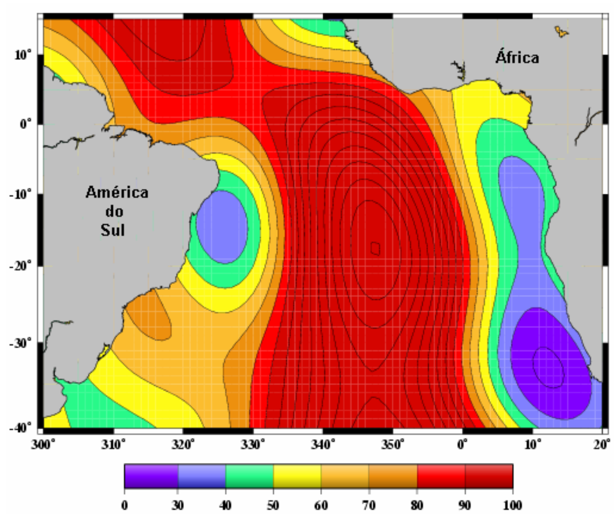

Figure (2) Regional heat flow map of the Equatorial region of the Atlantic Ocean, derived from the spherical harmonic coefficients of Pollack et al (1993).

Regional Trends in the global heat flow map of 2006

Recently Cardoso et (2005) carried out a reappraisal of global heat flow data and introduced corrections for a large number of apparent typographic errors in the database. In addition, an updated dataset was used for the South American continent. New sets of harmonic coefficients were calculated based on the revised data sets (Cardoso et al, 2005; Hamza et al, 2006). The procedure adopted here is quite similar to that employed by Chapman and Pollack (1975). Thus mean heat flow values were calculated for 5°x5° area elements. The grid system for which experimental data are available is illustrated in Figure (3). In this figure the red dots indicate grid elements for which experimental data are available. Similarly the white dots indicate grid elements for which estimated values based on empirical predictors were calculated. In this context it is perhaps worth pointing out that the use of empirical predictors was restricted exclusively to area elements for which experimental data are currently not available.

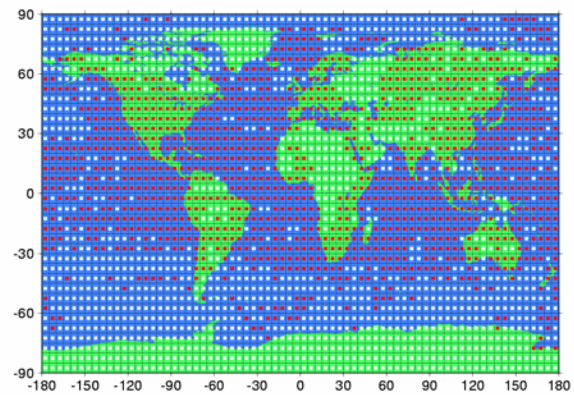

Figure (3) Grid system of 5°x5° surface area elements used for calculating mean heat flow over the globe. The red dots indicate grids for which experimental data are available. See text for details.

New sets of harmonic coefficients were calculated based on the revised data set for 12 and 36 degree harmonic expansions. The procedure adopted here is quite similar to that employed in the earlier works. However, we did not employ synthetic values, derived from plate cooling models, as substitute for experimental data.

In this context it is perhaps important to keep in mind the implications of the inverse relation between the degree of expansion and the spatial resolution. For example, the spatial resolution associated with 12 degree harmonic representation is only 15^0, which is equivalent to spatial dimensions of approximately 1600 km, in equatorial regions. On the other hand, 36 degree harmonic expansion has a spatial resolution of 5^0, which is better than 600km. Thus, the results of 12 degree representations presented in the earlier works of Chapman and Pollack (1975) and Pollack et al (1993) lacks the resolution for identifying heat flow anomalies with spatial dimensions of less than 15^0.

The new set of harmonic coefficients for the 36 degree expansion was also used in deriving the regional heat flow pattern in the equatorial region of the Atlantic Ocean. The results obtained are presented in the map of figure (4). In spite of the elimination of short wavelength variations the map based on the 36 degree harmonic expansion is able to reproduce the main heat flow anomalies along the mid ocean ridge system. The remaining parts of the oceanic regions and continental margins have heat flow values of less than 60 mW/m^2. In other words there is a much better agreement with the with the experimental data set and the mean values calculated in Table (1).

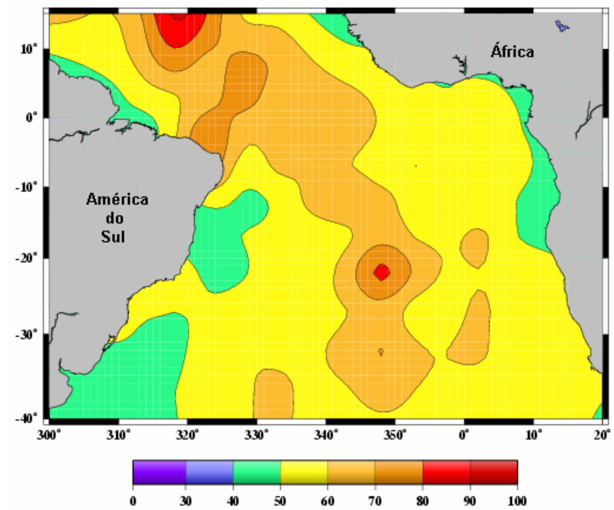

Figure (4) Regional heat flow map of the Equatorial region of the Atlantic Ocean, derived from the spherical harmonic coefficients of Hamza et al (2006).

Implications for the crustal thermal field of NE Brazil

The regional pattern inferred from harmonic analysis points to an elongated heat flow anomaly in the oceanic region adjacent to continental area of northeastern Brazil. An integrated analysis of heat flow values in both the oceanic and adjacent continental areas was carried out in an attempt to examine the nature of lateral dimensions of this anomaly. The results are presented in the map of figure (5).

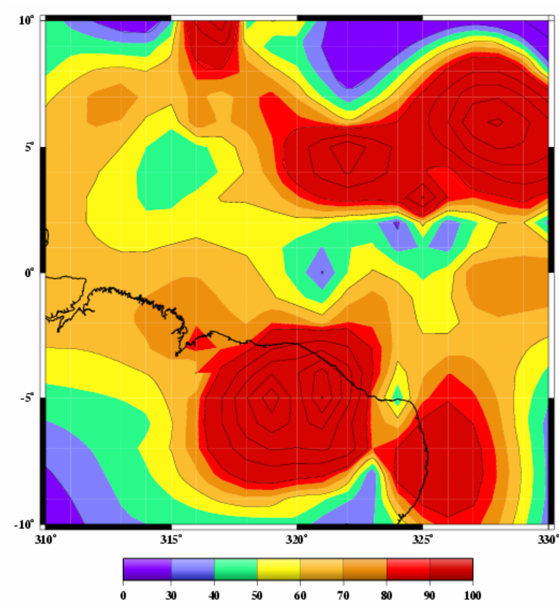

Figure (5) Regional heat flow map of the NE Brazil and adjacent oceanic region.

The map of figure indicates that the heat flow anomaly extends into interior of the state of Ceará and also covers much of the Potiguar rift basin.

Discussion

Obviously the major source of discrepancy between the set of mean values of Table (1) and the regional pattern of figure (2) arises from the widespread use of synthetic heat flow values calculated from plate cooling models. The practice of using theoretical values in place of experimental data is open to criticism as it is based on assumptions as to the nature of thermal processes at deeper levels in the crust, which is what we are trying to determine in the first place. Another problem with this procedure is that it requires extensive pre-processing of related geological and geophysical data. In many cases such information is not readily available, since detailed geologic mapping of ridge areas in oceanic regions have not so far been carried out. Also, the current level of knowledge about the tectonic and structural features in oceanic areas is far inferior to that in continental areas. Obviously such procedures are cumbersome and prone to errors, especially when large data sets are involved. Pollack et al (1993) selected 'suitable' values of tectonic age for the different sectors of ocean ridge areas and ignored the possibilities of alternative interpretations. In particular, the possibility that different sectors of ocean ridges could have distinctly different evolutionary history and geotectonic characteristics was not considered.

Acknowledgments

The first author of this paper received Masters Degree scholarship granted by Coordenadoria de Aperfeiçoamento de Pesquisa e Ensino Superior – CAPES, during the period of 2004-2006.

References

Birch, F., 1954, The present state of geothermal investigations, Geophysics, 19, 645 – 659.

Chapman, D.S. and Pollack, H. N., 1975, Global heat flow: A new look. Earth Planet. Sci. Lett.,28(1975), 23-32.

Lee, W.H.K., 1963, Heat flow data analysis, Rev. Geophysics., 1, 449-479.

Lee, W. H. K. and McDonald, G. J. F., 1963, The Global variation of terrestrial heat flow, J. Geophys. Res. 68, 6481 - 6492.

Lee, W.H.K. and Uyeda, S., 1965, Review of heat flow data, in Terrestrial Heat Flow, Geophys. Monogr. Ser., vol. 8, edited by W.H.K. Lee, pp. 87-100, AGU, Washington, D.C.

Jessop, A.M., Hobart, M.A. and Sclater, J.G., 1976, The world heat flow data collection – 1975, Geoth. Ser., vol. 20, Earth Physics Branch, Ener., Mines and Resources, Ottawa, Canada.

Hamza, V.M. and Muñoz, M., 1996, Heat flow map of South America, Geothermics, 25(6), 599-646.

Hamza, V.M. and Verma, R.K., 1969, Relationship of heat flow with the age of basement rocks, *Bull. Volcan*. **33**, 123-152.

Hamza, V.M., Soares, F.J.S. and Gomes, A.J.L. and Terceros, Z.D., 2005, Numerical and Functional representations of Regional heat flow in South America, Tectonophysics, v. 152, n. 4, p. 223-256

Pollack, H.N., Hurter, S.J. and Johnson, J.R., 1993, Heat flow from the Earth's interior: Analysis of the global data set, Reviews of Geophysics, 31, 3, 267 – 280.

Polyak, B.G. and Smirnov, Y.A., 1968, Relationship between terrestrial heat flow and tectonics of continents., *Geotectonics* (Eng. Transl.) **4**, 205-213.

Ponte Neto, C.F. and Hamza, V.M., 2004, Estimation of errors in spherical harmonic representation of global heat flow, Proceedings, Regional Symposium of the Brazilian Geophysical Society, São Paulo, 56-60.

Vasseur, G. and Nouri, Y., 1980, Trend of heat flow in France: Relation with Deep Structure. Tectonophysics, 65, 209-223.

Wessel, P. and Smith, W. H. F., 1998, New, improved version of Generic Mapping Tools released, *EOS Trans. Amer. Geophys*. U., vol. 79 (47), pp. 57

APPENDIX

The harmonic representation of heat flow (q) is usually expressed as:

$$q(\theta,\phi)=\sum_{n=0}^{N}\sum_{m=0}^{n}\left[A_{nm}\cos(m\phi)+B_{nm}\sin(m\phi)\right]P'_{nm}(\cos\theta) \quad (1)$$

where ϕ is the longitude θ = 90 – ψ, is the colatitude, $P'nm(\cos\theta)$ is the associated Legendre function that is fully normalized and A_{nm} and B_{nm} the coefficients of the harmonic expansion. The expression for evaluation of P'_{nm} is:

$$P'_{nm} = \frac{P_{nm}}{\sqrt{K_n^m}} \quad (2)$$

where P_{nm} is the associated Legendre function given by:

$$P_{nm}(\cos\theta)=\frac{\sin^m\theta}{2^n}\sum_{t=0}^{Int\left(\frac{n-m}{2}\right)}\frac{(-1)^t(2n-2t)!}{t!(n-t)!(n-m-2t)!}\cos^{(n-m-2t)}\theta \quad (3)$$

and

$$K_n^m=\frac{1}{H(2n+1)}\frac{(n+m)!}{(n-m)!}\ ,\ \begin{cases} if\ \ m=0\Rightarrow H=0 \\ if\ \ m\neq 0\Rightarrow H=2\end{cases} \quad (4)$$

In equation (3) *Int[(n-m)/2]* refers to the largest integer that is lower than *(n-m)/2*.

Full normalization of associated Legendre functions (P_{nm}) requires that the following equations be satisfied:

$$\int_0^{2\pi}\int_0^{\pi}\left[P'_{nm}(\cos\theta)\sin(m\phi)\right]^2\sin\theta\ \ d\theta\ \ d\phi=4\pi \quad (5a)$$

$$\int_0^{2\pi}\int_0^{\pi}\left[P'_{nm}(\cos\theta)\cos(m\phi)\right]^2\sin\theta\ \ d\theta\ \ d\phi=4\pi \quad (5b)$$